A

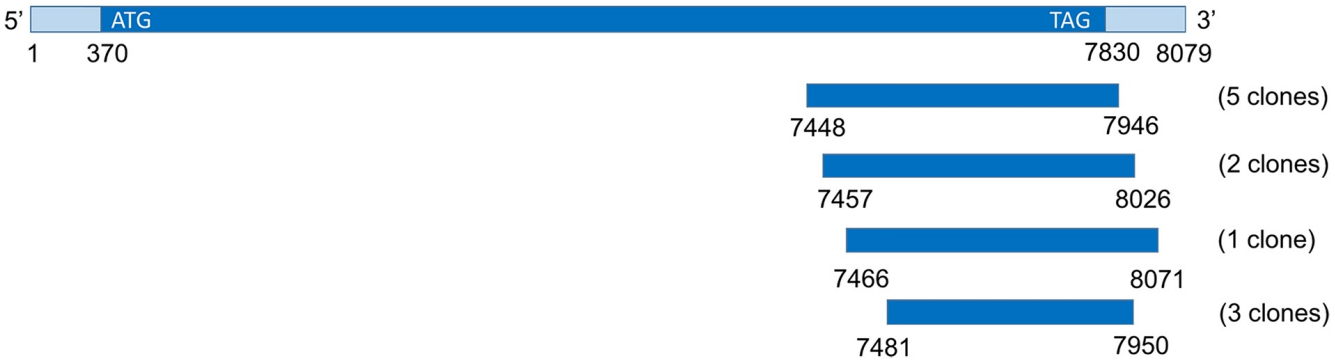

B

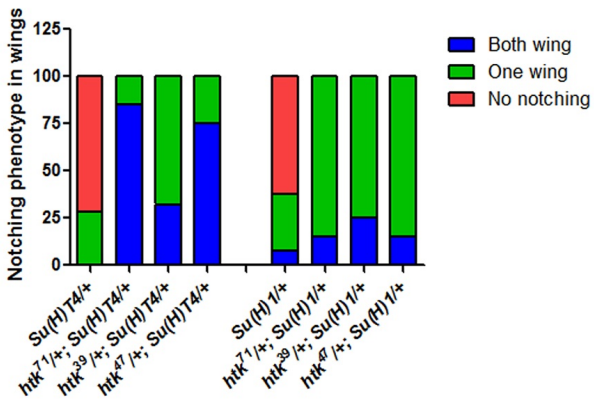

C

Genotype	Phenotypes (%)
+/+; ap-GAL4/+; UAS-htk-RNAi/+	Extra vein material near 2nd Cross Vein : 46% Defect in 2nd cross vein : 60% Extra row of bristles near wing margin : 34% 1st vein defective : 100% Patch of disorganized tissue at the tip of the vein : 60% Blisters in wing : 14% wings directed outward and upward : 100% Increased scutellar bristles : 72%
+/+; MS1096 –GAL4/+; UAS-htk-RNAi/+	Extra row of bristles near wing margin : 89% Patch of disorganized tissue at the tip of the vein : 72% Defect in 1st cross vein : 52%
+/+; +/+; C96 -GAL4 /UAS-htk-RNAi	Defect in 1st cross vein : 44% Extra vein : 12% Unusual bristle pattern : 39% Patch of disorganized tissue at the tip of the vein : 39%
+/+; ptc-GAL4 /+;UAS-htk-RNAi/+	Defect in 1st cross vein : 75% Patch of disorganized tissue at the tip of the vein : 52.5% Extra vein material near cross vein : 13% 1st cross vein very short and reduced intervein distance between L3-L4 : 100%
+/+; +/+; dpp-Gal4/UAS-htk-RNAi	Extra vein material near 2nd cross vein : 7.14% Patch of disorganized tissue at the tip of the vein : 49% Double 1st cross vein : 4%
+/+; en-GAL4/+; UAS-htk-RNAi	mis-oriented bristles and thinner wing blade in posterior region of wings : 75%
+/+; ey-GAL4/+; UAS-htk-RNAi	Reduced eye size :100%

D

Genotype	Phenotypes (100%)
+/+; ap-GAL4/+; UAS-HA-htk/+	• loss of scutellar bristles • reduced size of scutellum • severe wing blisters
+/+; en-GAL4 /+; UAS-HA-htk/+	• bending of third wing vein • thinner wing blade • incomplete fifth vein
+/+; ey-GAL4 /+;UAS-HA-htk/+	• loss of ommatidia
+/+; +/+; GMR-Gal4/UAS-HA-htk	• eye roughening

Figure S1: (A) Schematic representation of the sequence range of 11 positive yeast two-hybrid clones which overlapped with *htk* cDNA, when amino terminus of Notch-ICD (amino acids 1765–1895) was used as bait to screen 6x10^6 cDNAs from a *Drosophila* 0–24 h embryonic library. **(B)** Graph showing the frequency (number) of wing notching phenotypes observed in *Su(H)T4* and *Su(H)1* alleles individually and in trans-heterozygous combination with different *htk* alleles: *htk^{71}, htk^{39}, htk^{47}*. **(C)** Development defects induced by down-regulation of *htk* with a variety of GAL4 drivers, n=200. **(D)** Defects observed in wing and eye when ectopic expression of HA-*htk* was induced with a variety of GAL4 drivers, n=200. All phenotypes examined were 100% penetrant.

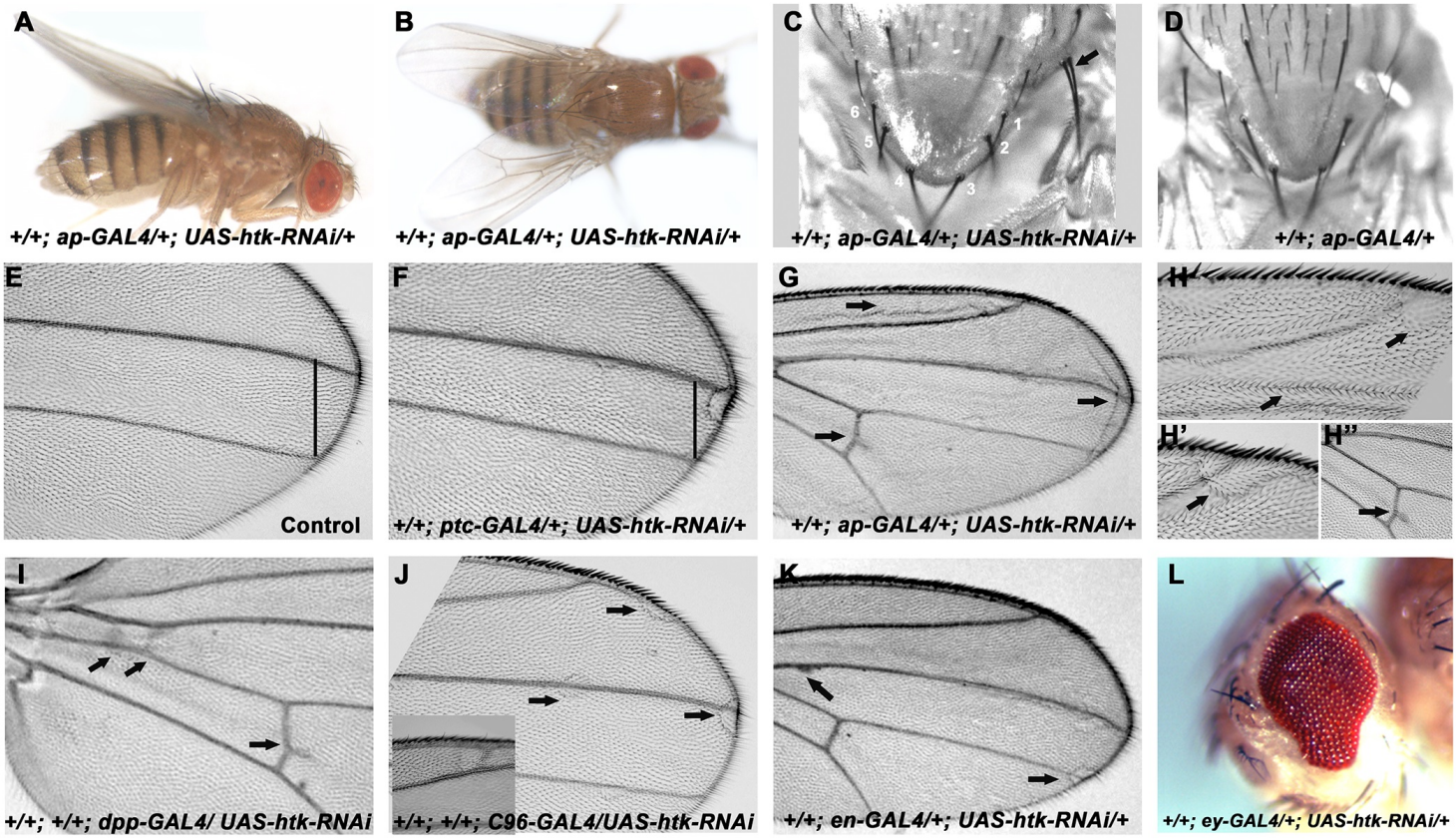

Figure S2: **Down-regulation of *htk* exhibits distinct phenotypes in *Drosophila* wings and eyes. (A-D, G)** *apterous-GAL4* driven *htk-RNAi* displayed upward (A) and outward (B) directed wings with extra rows of sensory bristles and vein material (arrow) in the wingblade (G), and increased scutellar bristles (C) compared to control (D). Similarly when *htk* was down-regulated at anterior-posterior boundary using *patched-GAL4* **(F)** and *dpp-GAL4* **(I),** at wing margin using using *C96-GAL4* **(J)**, in posterior compartment of wing using *engrailed-GAL4* **(K)**, and in the eye using *eyeless-GAL4* **(L)**, it resulted in reduced distance between L3 and L4 veins (black line) **(F)**, extra vein material (arrows) **(I)**, areas with thinner cuticle (arrows) **(J, K)** and reduced eye-size **(L)**, respectively. **(E)** Control adult wing displaying normal wing margin and longitudinal veins L1–L5. **(H-H")** High magnification images of wing showing extra row of bristles (H), area with thinner cuticle (H'), and extra vein material (H''). Several htk down-regulation phenotypes mimic Notch loss-of-function phenotypes.

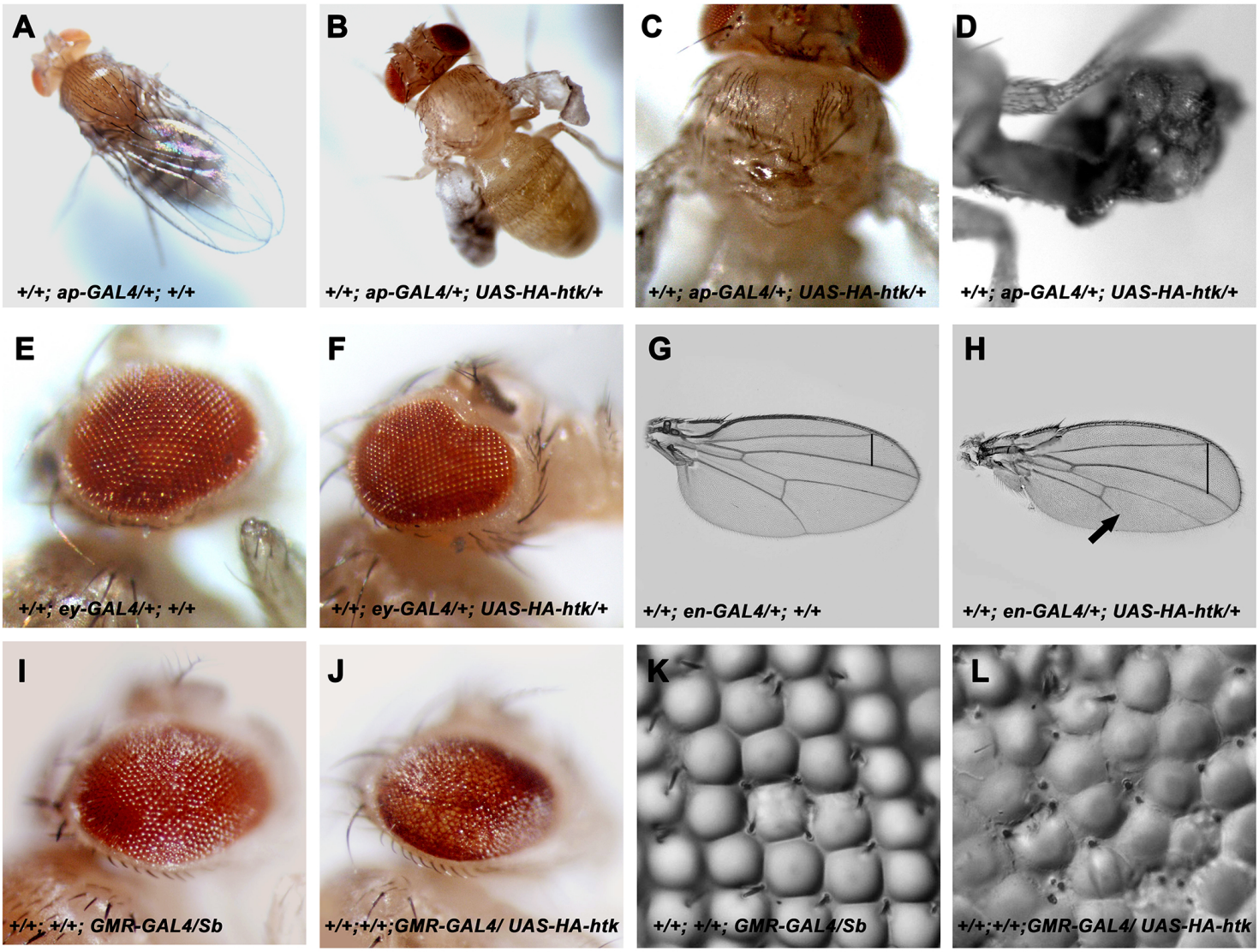

Figure S3: **Over-expression of *htk* resembles *Notch* gain-of-function phenotypes. (A-D)** Ectopic expression of *htk* driven by *apterous-GAL4* causes loss of scutellar bristles **(B, C)** and deformed wing **(B, D)** in comparison to only *apterous-Gal4/+* fly **(A)**. **(E,F)** *eyeless-GAL4* driven expression of *htk* in eye results in loss of ommatidia. **(G,H)** Over-expression of *htk* in posterior region of wing using *engrailed-GAL4* results in incomplete fifth vein and increased inter-vein distance between second and third vein. **(I, J)** Ectopic expression in adult eye using *GMR-GAL4* results in increased eye-roughening and loss of ommatidial bristles. **(K, L)** Nail polish imprint images of adult eye showing these eye phenotypes more clearly. Phenotypes showed 100% penetrance.

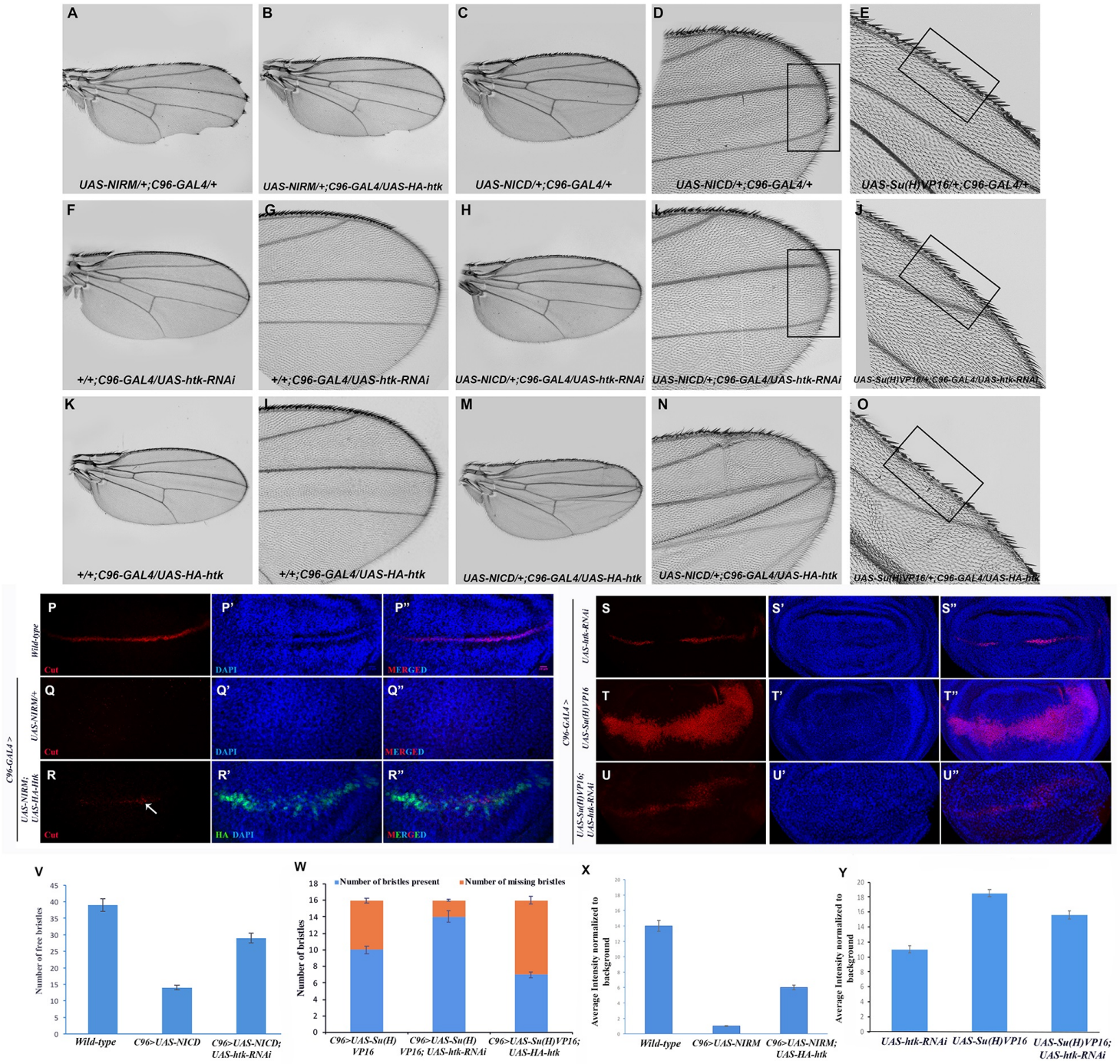

Figure S4: Epistatic interactions of *htk* with Notch pathway. *C96-GAL4* was used to drive the expression of different *UAS* lines at wing margin. **(A-O) Wing images showing epistatic and synergistic interactions between *htk* and *Notch* or *Su(H)VP16***. No notching or bristle irregularities were observed when *htk* was downregulated (F, G), or upregulated (K, L) at the wing margin. When the dose of *htk* was increased in *Notch* loss-of-function background, the wing notching phenotype caused by *Notch-RNAi* (A) was significantly rescued (B). Over-expression of *Notch* (C, D) and *Su(H)VP16* (E) at the wing margin resulted irregularities in wing bristle. This irregularity in bristle pattern was rescued when dosage of *htk* was reduced in this background (H-J). The irregularity in bristle localization was quantified by counting the number of free bristles in the same selected area of wing (n=10) expressing *Notch-ICD* alone and *Notch-ICD* along with *htk-RNAi* (boxed regions, 350µm length) **(V)**, and by counting the number of thick dorsal bristles present or absent in the same selected area of wing expressing *Su(H)VP16* alone and *Su(H)VP16* along with *htk-RNAi* (boxed region, 200µm length) **(W) [**error bars indicate standard error of the mean (n=3)]. The quantification is represented as the graph. Additionally, when *htk* along with *Notch* or *Su(H)VP16* were co-expressed, an increase in the wing margin irregularities was observed (M-O). All the phenotypes showed 100% penetrance (n=100). **(P-U'') Activity of Notch signaling was observed during epistatic interaction of *htk* with *Notch* and *Su(H)VP16***. Notch downstream marker, Cut was used to report the Notch signaling activity. DAPI marked the nuclei. The wild type Cut expression (P) was lost when Notch was reduced at dorso-ventral boundary of wing disc (Q). A rescue in the Cut expression was observed when *HA-htk* was over-expressed in the same background (R). (S-U'') Alternatively, ectopic expression of Cut caused by over-expression of *Su(H)VP16* (T) was partially rescued when *htk* was reduced in this background (U). Images in third column in both the panel are merged of images from first and second column. **(X, Y)** Quantification of Cut signal intensity at dorso-ventral boundary of wing disc is represented in the form of a graph. Cut signals are normalized to background signals, and values relative to controls are presented. Error bars indicate standard error of the mean (n=3). Figure D, G, I, L, N are higher magnification images of C, F, H, K, M, respectively. Scale bar, (P-U'') 10µm.

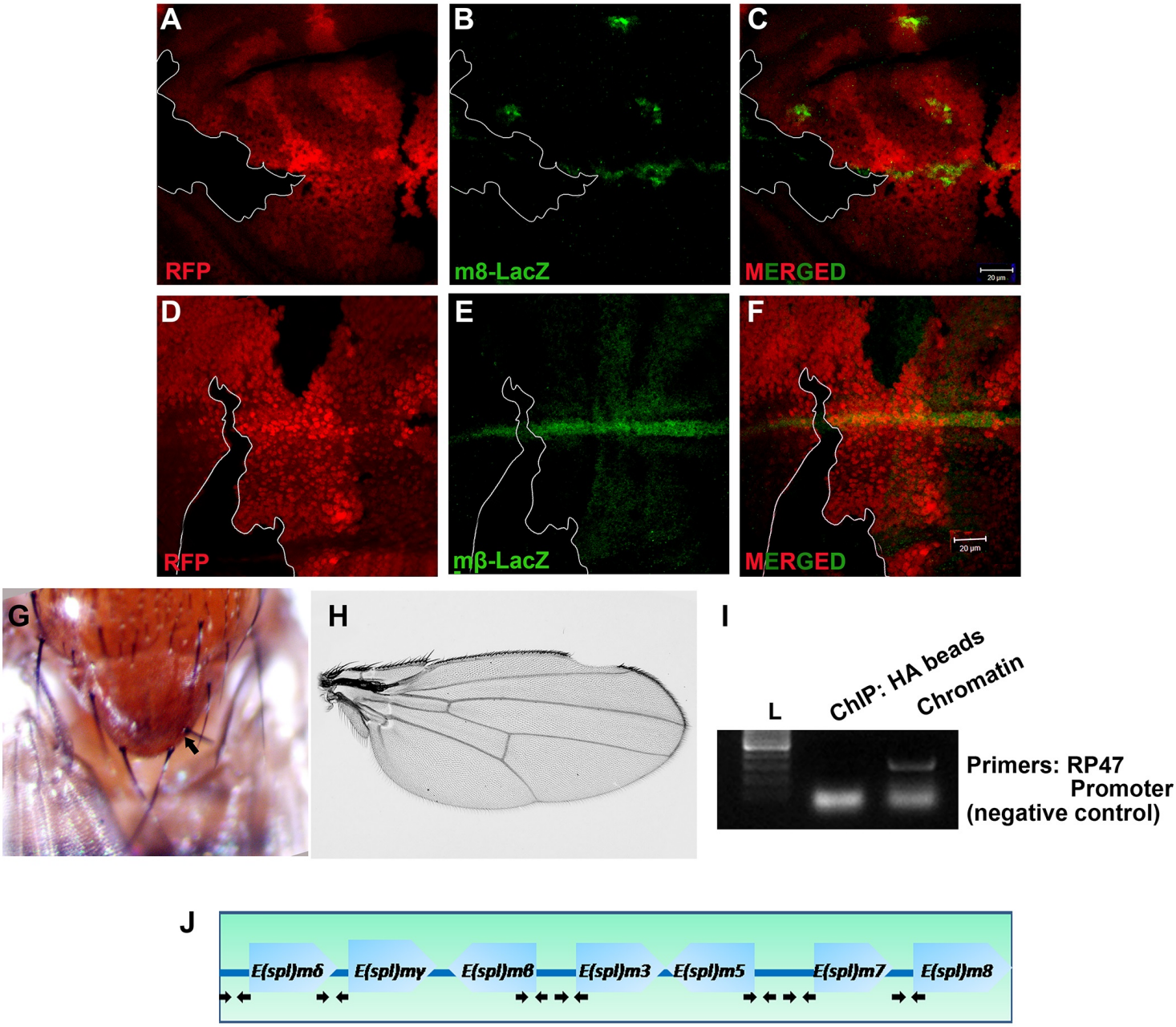

Figure S5: *htk* regulates Notch signaling activity. (A-F) Loss-of-function clones of *htk* displayed reduced expression of *E(spl)* complex genes. **(A, D)** *htk* mutant somatic clones were marked by absence of RFP expression. **(B, E)** The LacZ reporter stocks were used to verify *E(spl)m8* and *E(spl)mβ* expression (shown in green)**.** Third column images are merges of those in first and second columns. The expression of Notch downstream targets, *E(spl)m8* **(A-C)** and *E(spl)mβ* **(D-F)** was significantly reduced in *htk* loss-of-function clones. Scale bar, 20 µM. **(G-H)** Adults developed from larvae containing *htk* loss-of-function somatic clones, displayed various developmental defects such as increased scutellar bristles **(arrow, G),** notching at wing margin **(H),** etc. These phenotypes are also Notch loss-of-function phenotypes. **I.** Agarose gel electrophoresis image for negative control showing that Htk could not immunoprecipitate promoter of *RPS 49* gene. PCR using primers specific for promoter of *RPS 49* gene shows no positive amplification from template DNA fragments which was immunoprecipitated with Htk protein (Lane2). Chromatin samples before immunoprecipitation contain all the genomic DNA fragments, and were used for positive control (Lane 3). **J.** Schematic picture representing the localization of the primers used for ChIP experiment.

Table S1. Primers for RT-qPCR

mβ_RT_Fw 5'- ACCGCAAGGTGATGAAGC -3'
mβ_RT_Re 5'- CTTCATGTGCTCCACGGTC -3'
mδ_RT_Fw 5'- ATGGCCGTTCAGGGTCAG -3'
mδ_RT_Re 5'- CCATGGTGTCCACGATG -3'
mγ_RT_Fw 5'- GTCCGAGATGTCCAAGAC -3'
mγ_RT_Re 5'- GACTCCAAGGTGGCAACC -3'
m3_RT_Fw 5'- ATGGTCATGGAGATGTCC -3'
m3_RT_Re 5'- GCACTCCACCATCAGATC -3'
m5_RT_Fw 5'- ATGGCACCACAGAGCAAC-3'
m5_RT_Re 5'-TGTCCATTCGCAGGATGG -3'
m7_RT_Fw 5'- GGCCACCAAATACGAGATG -3'
m7_RT_Re 5'- CAT CGC CAG TCT GAG CAA -3'
m8_RT_Fw 5'- GGAATACACCACCAAGACC -3'
m8_RT_Re 5'- CGCTGACTCGAGCATCTC -3'

Table S2. Primers for promoter regions

m3_Fw 5’-GATCCAATCCGAAAGCCG-3’
m3_Re 5’-CTAGTTCCCAGCCCTACT-3’
m5_Fw 5’-GTGGTTGTCTGTGTGGAG-3’
m5_Re 5’-GACCTGCTACCTGCGAACA-3’
m7_Fw 5’-GCACGCATGTTCCGTTTG-3’
m7_Re 5’-GGGAAACACTTTGCCCTC-3’
m8_Fw 5’-GCCAATATGCCACATCCAC-3’
m8_Re 5’-GGAACAGCTGCAACTTCG-3’
mβ_Fw 5’-ACTTCGATCGGTTCCCAG-3’
mβ_Re 5’-GAACTGGACAGTGAGTGC-3’
mδ_Fw 5’-GCGGCACAATCCCAATAC-3’
mδ_Re 5’-CTGGTTCCCACTTCCCT-3’
mγ_Fw 5’-CACTCCGTTTACAAATCCCTG-3’
mγ_Re 5’-GCTAGACCTTCGGTGATC-3’